Conduction mechanisms in carbon-loaded composites

1996 J. Phys.: Condens. Matter 8 8321

(http://iopscience.iop.org/0953-8984/8/43/024)

J. Phys.: Condens. Matter **8** (1996) 8321–8338. Printed in the UK

Conduction mechanisms in carbon-loaded composites

J C Dawson and C J Adkins

Cavendish Laboratory, Madingley Road, Cambridge CB3 0HE, UK

Received 24 July 1996

Abstract. Results on the conductivity as a function of temperature of carbon black–polymer composites with a wide range of loadings are presented and discussed. Inter-particle transfers dominate the resistivity in the low-loading composites, and the conductivity is described quantitatively by the theory of fluctuation-induced tunnelling. This mechanism together with orbit shrinkage accounts for the observed positive magnetoresistance. In the highly loaded composites the conduction mechanism within the carbon black becomes important. This is found to be well described by theories of two-dimensional conduction in a disordered metal. The two-dimensional nature results from the graphite layered structure of carbon black. The magnetoresistance of the highly loaded composites is also found to be positive and quantitatively consistent with resulting from interaction effects. We are unable to explain the apparent suppression of the weak-localization contribution to their magnetoresistance.

1. Introduction

Carbon-black-loaded polymers are used in industry as anti-static materials; however, the conduction mechanisms are not fully understood. In this paper a wider range of loadings are examined than in previous work, and a novel explanation of the conductivity at high loadings is provided. The paper begins with a description of the structure of these materials followed by details of the experiments and a discussion of previous work. The measurements of resistance as a function of temperature and of magnetoresistance are then presented and discussed.

Comparing the x-ray diffraction pattern of a carbon black with that of polycrystalline graphite, the carbon black peaks are found to correspond roughly to the positions of the graphite (002), (100), (004) and (110) peaks. The absence of the graphite $(hk\ell)$ $(\ell \neq 0)$ peaks indicates a lack of three-dimensional ordering. Thus the structure consists of graphite planes stacked approximately parallel to each other, but each layer is randomly rotated with respect to the next—a *turbostratic structure*. In addition the (00ℓ) peaks are shifted to lower values than in graphite, indicating a larger inter-plane distance.

The model originally proposed for the structure of the basic carbon black unit was of small turbostratic crystallites joined together by disordered carbon (Warren 1941). However, electron microscopy does not support the presence of such small crystallites (Ergun 1970). Instead, it appears that the graphite planes at the periphery of the particles form approximately spherical concentric shells. The carbon in the centre may be more disordered. In a highly structured black such as that studied here the individual carbon black units fuse together permanently during manufacture to form large aggregates; the graphite layer planes are continuous between the particles (Burgess *et al* 1971). The two models are illustrated in figure 1.

0953-8984/96/438321+18$19.50

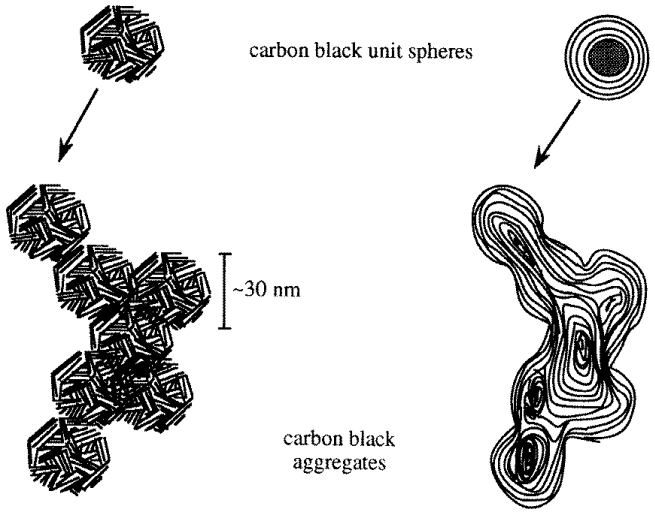

Figure 1. A schematic depiction of carbon black structure. The lines indicate the graphitic planes. The left-hand diagram corresponds to the original small-crystallite model, the right-hand one to the 'continuous shells' structure.

A carbon-loaded polymer is a conductor–insulator mixture, and exhibits a percolation threshold (figure 2). As such it resembles a conventional granular metal. However, there are important differences. The first concerns the average conducting particle size in systems below the percolation threshold. In a carbon–polymer composite this is set by the size of the fused carbon black aggregates, which is typically 0.1–2 μm. This size does not vary with loading. In a granular metal, average metal island sizes vary and are typically in the range 1–10 nm. Thus, in a granular metal, island charging energies (which scale inversely with particle size) are significant, while they are negligible in a carbon black composite.

The second difference is on the other side of the percolation threshold. In a granular metal the islands coalesce at high enough loading, forming metallic paths through the matrix. Carbon black particles do not coalesce, though they will touch. At high loadings, transfer between particles becomes easy and the resistivity of the carbon black particles themselves must be considered. A single graphite sheet is a zero-band-gap semiconductor while graphite is a semi-metal (Robertson 1986). The conductivity is also highly anisotropic, with the in-plane conductivity 2–3 orders of magnitude greater in crystalline graphite than that perpendicular to the planes.

Table 1. Details of composites studied. The resistivities were measured at room temperature.

Material	% carbon black by volume	Resistivity/Ω m	Matrix
C-wax	50	8.1×10^{-4}	Montan wax
EC140	15	3.4×10^{-1}	Polycarbonate
EC099	6	2.4×10^{4}	Polycarbonate
EC097	5	4.3×10^{8}	Polycarbonate

The materials discussed in this paper are listed in table 1. They were provided by ICI Wilton Materials Research Centre, and were made using XC72 carbon black. This black

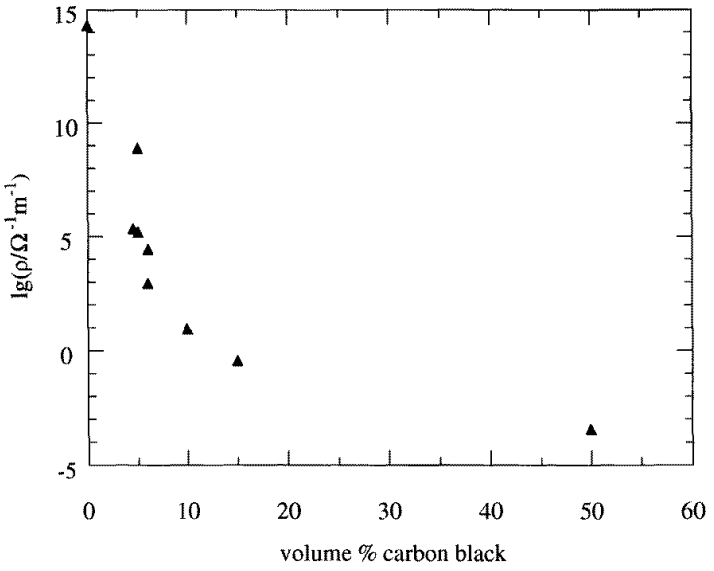

Figure 2. Composite resistivity as a function of XC72 carbon black loading. The matrix of the 50%-loaded material is Montan wax, that of all others polycarbonate. The resistivity of pure polycarbonate is taken from Bolz and Tuve (1973).

consists of 30 nm diameter spherical particles fused into aggregates up to 2 μm long. The highly extended nature of the aggregates facilitates the formation of a conducting network when dispersed in a polymer. The polycarbonate samples were prepared by melt processing at 530 K for 20 minutes followed by compression moulding at 500 K to form sheets about 0.3 mm thick which could be cut with a scalpel. The 50%-loaded sample was compacted at 295 MPa and 373 K (above the melting point of the Montan wax matrix) and then cooled to room temperature while still under pressure, producing a disc about 3 mm thick from which a rod was milled.

2. Experimental techniques

The resistance of the materials was measured as a function of temperature using an Oxford Instruments CF200 continuous-flow cryostat from room temperature to 6 K, and a pumped ^{4}He cryostat from 4.2–1.2 K. The latter also contained a BOC Superconducting Magnet Systems 5T magnet for magnetoresistance measurements. For the two least conductive materials, a two-terminal dc method was used. A four-terminal ac method was used otherwise, except on EC140 at low temperatures where unavoidable system capacitances required the dc technique. (ac and dc methods agreed at higher temperatures.) In all cases electrical contact was made to the materials using silver paint.

3. Previous work

Measurements of the temperature dependence of the resistivity of carbon-loaded composites have been published and interpreted by a number of groups. However, no theory has yet

been successful in accounting for all the results obtained. This may partly result from the variety of hosts used for the carbon black; but most models assume the matrix to act simply as an inert spacer for the carbon so it is not unreasonable to expect some uniformity of behaviour. Resistance is generally assumed to be dominated by transfer of charge across the insulating gaps between carbon black particles.

Near room temperature many composites show an increase in resistance with temperature. This is explained qualitatively by the fact that the matrix has a much larger thermal expansivity than the carbon so, as temperature is increased, the matrix expands relative to the carbon and the effective volume loading decreases. Attempts by Ohe and Naito (1971) and Al-Allak *et al* (1993) to describe this quantitatively proved unsuccessful due to the oversimplified models they used.

At lower temperatures the resistance increases with decreasing temperature. The theory of fluctuation-induced tunnelling conduction (Sheng *et al* 1978) is used by Sichel (1982) and Ezquerra *et al* (1986) to describe their results. In this model conduction occurs via tunnelling across small tunnel junctions between carbon black particles. The junction area and its capacitance are very small and so thermal voltage fluctuations across it are important. This leads to a temperature-dependent expression for the tunnelling conductivity which reduces to simple activation at high temperatures and to temperature-independent tunnelling at low temperatures. The theory provides a reasonable fit to their data below 100 K, although their chosen tunnel junction barrier height of 0.2 eV is rather low. Fabish and Schleifer (1984) found little difference between the contact potentials of carbon black and gold, and thus a typical metal–insulator barrier height of about 1 eV would appear more likely.

Mehbod *et al* (1987) used a critical path method (Sheng and Klafter 1983) to describe their results on highly insulating composites. The theory provides a reasonable fit to the data, but relies on there being an energy-dependent density of states. Such a density of states can be produced by a distribution of charging energies (Adkins 1982). However, as pointed out earlier, the charging energy of a carbon black particle is negligible due to its size. No other justification for the form of the density of states was offered.

Van der Putten *et al* (1992) interpreted their results on composites above the percolation threshold as due to variable-range hopping on a fractal network. On such a one-dimensional network, wave functions are supposed to become 'superlocalized', decaying faster than exponentially with distance, so leading to a modified exponent in the variable-range-hopping expression (Deutscher *et al* 1987). The value of the superlocalization exponent which they derive from their results is not however consistent with the currently accepted figure (Aharony *et al* 1993). A further objection to their use of this theory is that the derived optimum hop distance is not always greater than the localization length which again is not consistent with the model.

This brief review of previous work shows that the mechanisms controlling resistivity in carbon-loaded composites are still not properly understood.

4. Conductivity results

As the materials studied here show large differences in behaviour (see figure 3) the results will be discussed in three subsections—the 5%- and 6%-loaded materials first, followed by that with a loading of 15%, and finally the 50%-loaded sample.

In composites with low carbon black loadings (the 5%-, 6%- and 15%-loaded samples studied here) resistance is dominated by the transfer of electrons between particles. The novel suggestion resulting from our work is that in much more highly loaded materials the variation of the sample conductivity with temperature is instead due to the transport process

within the carbon black particles. This transport can be described using theories derived for conduction in disordered electronic systems, with the assumption that, due to the planar graphitic structure, electrons are essentially confined to two dimensions in the carbon black, despite the fact that the system as a whole is three dimensional. This interpretation differs from the work described in the previous section, in which the carbon black particles are effectively assumed to be perfect conductors. Our new interpretation will be discussed in more detail when our results for highly loaded composites are presented.

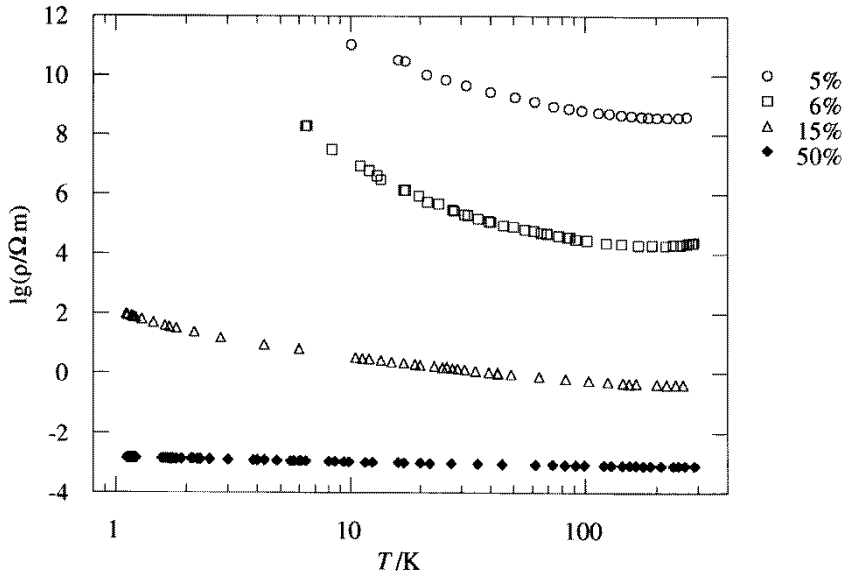

Figure 3. Resistivity as a function of temperature for carbon-loaded composites.

4.1. Results with lightly loaded composites

The resistivity of the two least conducting materials could not be measured using a four-terminal technique due to the difficulty in making good electrical contact to them. The possibility of significant contact resistances must therefore be considered. Norman (1970) discusses this problem in his book on conductive rubbers and plastics and reports a wide variation in the efficiency of different electrode materials. Silver paint is described as 'good'. Ezquerra *et al* (1986) also found only small contact resistances with silver paint electrodes. Silver paint was used in our measurements and as the materials themselves are so resistive it is expected that any contact resistance is negligible in comparison.

The conductivity of the composites exhibits a maximum around 200 K, shown clearly in figure 4. This is due to the different thermal expansivities of the two components: the expansivity of carbon is $\sim 2.5 \times 10^{-6}$ K^{-1} whereas that of polycarbonate is $\sim 6.6 \times 10^{-5}$ K^{-1} (Bolz and Tuve 1973). Thus, as the temperature increases the matrix expands and the carbon black particles move further apart, causing the resistance to rise. The effect is most noticeable in the 5% and 6% materials as in this range the resistance is extremely sensitive to small changes in the loading.

Below 200 K the resistivity increases dramatically with decreasing temperature. In this

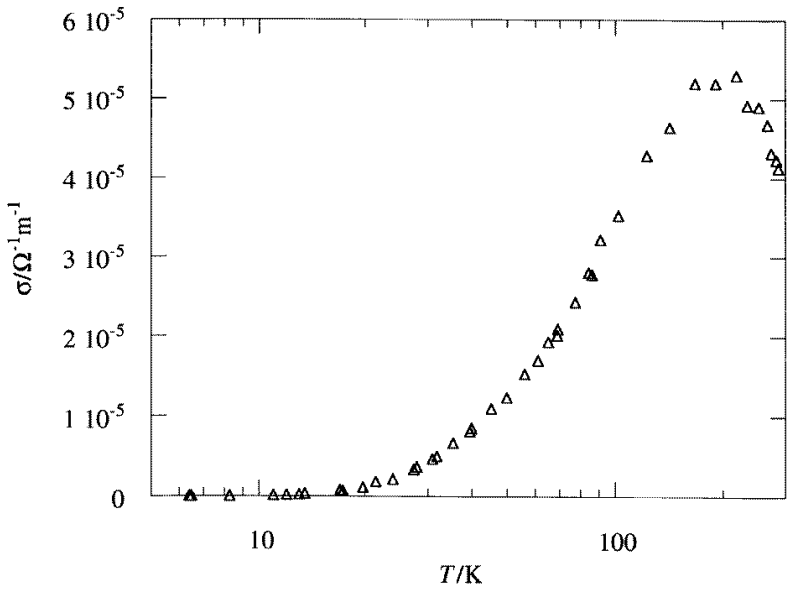

Figure 4. A plot of conductivity versus temperature for EC099 (6%) with the maximum at ∼200 K clearly visible.

regime the theory of fluctuation-induced tunnelling conduction (Sheng 1980) was found to describe the data best. This theory was developed specifically to explain the conductivity of carbon-loaded composites and takes account of the large size of the particles. In examining our data, we used the simplest form, assuming a parabolic barrier and single-junction characteristics. In this case the conductivity is expected to behave as

$$\sigma(T) = \sigma_0 \exp\left[-T_1/(T + T_0)\right] \tag{1}$$

with T_1 and T_0 being related to the median values of the junction parameters in the system. A least-squares fit to equation (1) was made to the data below 200 K to obtain the values of T_1 and T_0 for each sample. The results are shown in figures 5 and 6 and the fitting parameters are listed in table 2.

Table 2. Fitting parameters for fluctuation-induced tunnelling. The errors are those obtained from the least-squares analysis.

Material	Loading/%	$\sigma_0/\,\Omega^{-1}\mathrm{m}^{-1}$	T_1/K	T_0/K	αd
EC097	5	5.6×10^{-9}	158 ± 2	15.0 ± 0.3	6.7
EC099	6	8.0×10^{-5}	100 ± 2	4.0 ± 0.2	15.9

The product αd, where α is the tunnelling exponent and d the tunnelling distance, can be obtained from the ratio T_1/T_0, giving $\alpha d = 15.9$ for EC099 and 6.7 for EC097. These are both much greater than 1, as required for a tunnelling mechanism. However, we might have expected the more resistive material EC097 to have the larger αd, whereas the reverse is found here. Figure 6 also shows the fit to EC097 using the parameters derived from the EC099 fit. This provides as good a fit to the data at temperatures greater than 10 K as the free fit does. The sample resistance at 10 K was extremely high and that measurement

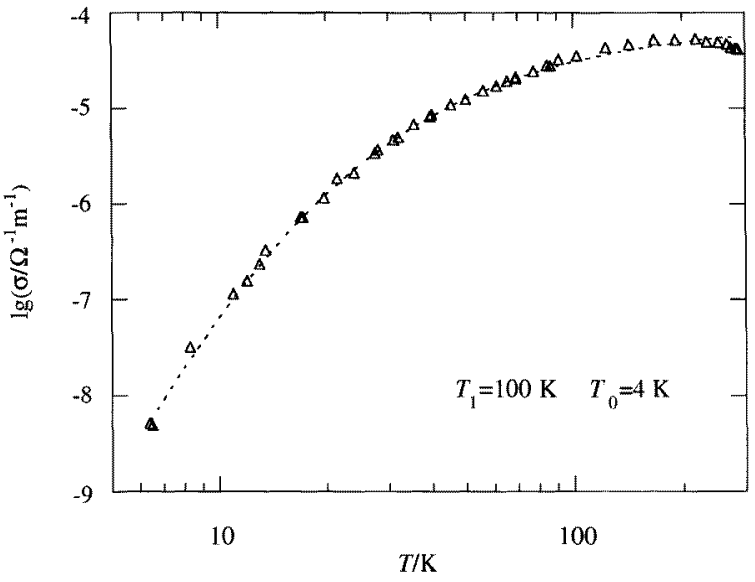

Figure 5. A fit to the theory of fluctuation-induced tunnelling conduction for EC099 (6%).

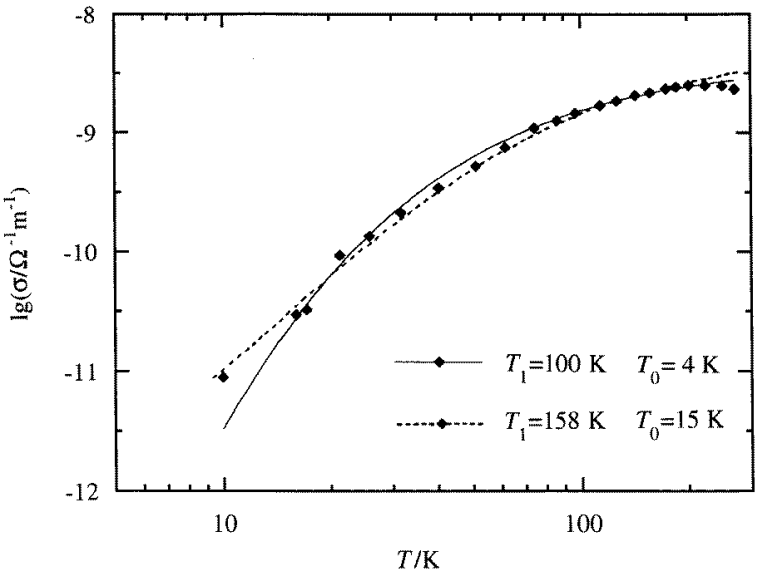

Figure 6. Fits to the theory of fluctuation-induced tunnelling conduction for EC097 (5%). The dashed curve is the result of a free fit; the full line is the curve given by the parameters deduced from the EC099 fit with $\sigma_0 = 4 \times 10^{-9}\ \Omega^{-1}\ \mathrm{m}^{-1}$.

may therefore not be very reliable. Thus the values of T_1 and T_0 derived from the EC099 fit will be used to describe both materials, the difference in the absolute resistivities being accounted for by differing values of the pre-exponential factor σ_0. The expression (1) is

valid for $T < 2T_1$ (Sheng *et al* 1978), a condition which is met here since the fits were only performed for $T < 200$ K.

Three parameters are involved in T_1 and T_0: the tunnel junction width d, area A and barrier height V_0. Table 3 lists the values of d and A obtained when V_0 is chosen as indicated. The value of $\epsilon_r = 3.17$ used is that for polycarbonate (Brydson 1982), as this is the intervening material through which the electron must tunnel.

Table 3. Junction parameters for various values of V_0.

V_0/eV	d/nm	A/m^2
4	1.5	5.7×10^{-22}
2	2.2	3.5×10^{-21}
1	3.1	1.9×10^{-20}
0.75	3.6	3.8×10^{-20}
0.5	4.4	1.1×10^{-19}

The junction areas are small, indicating that tunnelling takes place between protruding atoms. Since the tunnelling probability falls off exponentially with distance small areas are expected.

Tunnelling distances of the order of nanometres are reasonable, although those associated with the small barrier heights are rather large. These are simply estimates of the size of a typical junction, assuming that it can be modelled as a parallel-plate capacitor; the real system will contain a range of junctions with varying parameters. The derived parameters are therefore reasonable, with barrier heights of the order of an electron volt being most likely. Thus this theory allows a quantitatively consistent interpretation of the data.

4.2. Results with a 15%-loaded composite

The resistivity of EC140 (15%) was measured as a function of temperature and pressure (up to 22 kbar). In addition magnetoresistance measurements were made. Attempts to measure the Hall effect were unsuccessful, probably due to the granular nature of the material in which conduction occurs along percolation paths.

4.2.1. Resistivity measurements. The 'high'-temperature (i.e. $T > 5$ K) results on EC140 will be presented first. The usual measurement of resistance as a function of temperature was augmented in this case by measurements of the variation of resistance with pressure. The apparatus used is described by Parker (1988). The sample resistance was measured using a four-terminal ac technique.

Figure 7 is a plot of conductivity as a function of temperature (>5 K) for EC140 at various applied pressures. The results were reversible with respect to temperature. The curves are the best fits to the fluctuation-induced tunnelling conduction equation (1). The fitting parameters are listed in table 4.

T_1/T_0 shows the expected trend, decreasing with increasing pressure (corresponding to decreasing αd). As mentioned earlier, the form (1) is only valid for $T < 2T_1$. The fits here were based on data below 200 K to avoid any interference from thermal expansion differences, and this inequality is satisfied over most of the range. σ_0 increases with pressure, corresponding to more percolation paths becoming available. The last two columns of table 4 give the junction areas A and widths d obtained assuming a barrier height of 1 eV and that the junctions can be modelled as parallel-plate capacitors. These junction parameters are

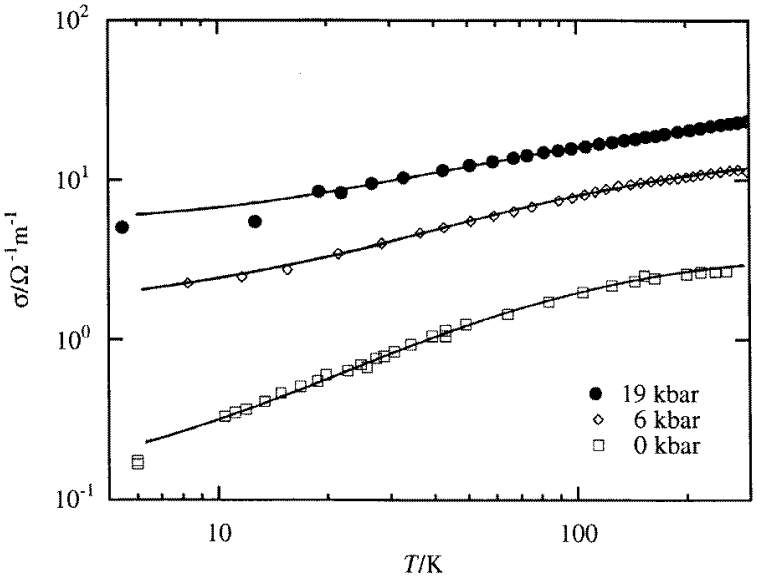

Figure 7. Fluctuation-induced tunnelling fits to EC140 at various applied pressures.

Table 4. Fitting parameters for fluctuation-induced tunnelling for EC140 and derived junction dimensions

Pressure/kbar	$\sigma_0/\Omega^{-1}\ m^{-1}$	T_1/K	T_0/K	T_1/T_0	d/nm	A/m^2
0	3.8 ± 0.1	82 ± 4	23 ± 2	3.6	0.44	2.2×10^{-21}
6	15.65 ± 0.08	98 ± 1	42.2 ± 0.7	2.32	0.29	1.7×10^{-21}
19	27.2 ± 0.2	78 ± 2	46 ± 2	1.7	0.21	1.0×10^{-21}

rather small, but, as in the case of the lightly loaded composites, too much significance should not be attached to them: the fact that the ratio T_1/T_0 gives consistent and reasonable values of αd is the best indication that the theory can be used here.

At temperatures $T \ll T_0$ the fluctuation-induced tunnelling mechanism reduces to a temperature-independent tunnelling process. However, the resistance of EC140 continues to increase with decreasing temperature well below T_0. The resistivity at these temperatures is too high for it to be accounted for by the intra-particle process discussed in the next section, nor is the temperature dependence of the correct form. The continuing increase in resistivity below T_0 must therefore still be due to the inter-particle transfers. It may simply be a result of the distribution of junction parameters within the material. The temperature dependence observed at low temperatures is then due to the gradual 'freezing out' of the fluctuation-induced tunnelling process, starting with the junctions with highest T_0.

The variation of the room temperature resistance of EC140 as a function of pressure is shown in figure 8. As might be expected, the resistance decreases with increasing pressure, as the conducting particles are forced closer together. If conduction is dominated by tunnelling through the insulating gaps separating the carbon black particles, the expected change with pressure p, assuming that all the tunnel junctions are identical, is given by

$$R(p)/R(0) = \exp(-2\alpha\ \Delta d) = \exp(-2\alpha p d/3B)$$

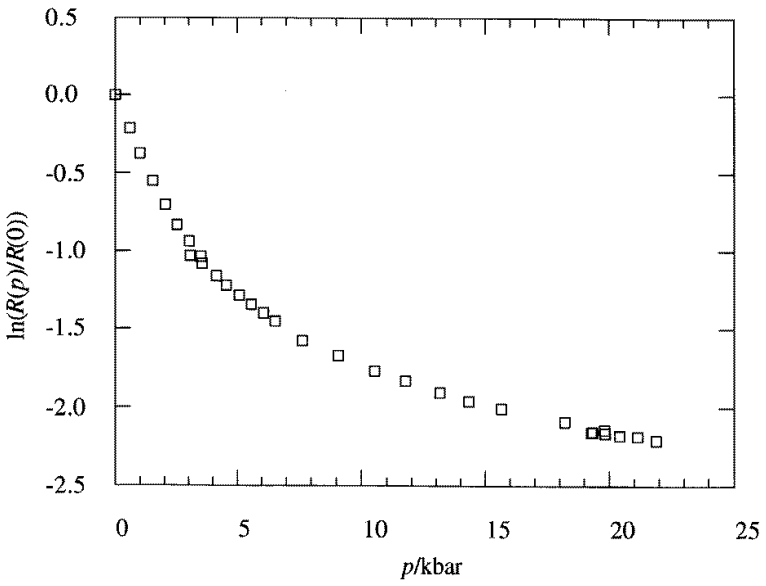

Figure 8. The logarithm of normalized resistance versus pressure for EC140 at room temperature.

where α is the tunnelling exponent, d the tunnelling distance and B the bulk modulus. Thus the plot of $\ln(R(p)/R(0))$ versus p should be a straight line of slope $-2\alpha d/3B$. We see from figure 8 that the dependence is not linear over the range of measurement. However, a straight line can be fitted to the low-pressure data ($P < 2.5$ kbar) and has a slope of -0.34 kbar^{-1}. Using the bulk modulus of polycarbonate, 7.58×10^7 Pa (Bolz and Tuve 1973), this corresponds to $\alpha d = 0.39$. This is not consistent with the tunnelling premise for which we must have $\alpha d > 1$.

The above analysis is oversimplistic, however, as it assumes the whole material is compressed uniformly. In fact, the compressive strength of the carbon is 5–10 times lower than that of polycarbonate (Bolz and Tuve 1973) so the inhomogeneous material will not compress uniformly. In particular, since the carbon is much more easily compressed, the stress in the polycarbonate in the small gaps between carbon particles (where the tunnelling occurs) will be largely relieved and the local strain will be much smaller than if the material compressed uniformly. The effective 'bulk modulus' for the tunnelling region is thus much increased. This results in much larger calculated values of αd so satisfying the requirement $\alpha d > 1$.

The effect of differing moduli can be illustrated by considering the two components as fluids and subject to uniform hydrostatic pressure. It is then easily shown that the small gaps between carbon 'droplets' can actually *increase* in width with applied pressure when the moduli are sufficiently different. The required difference depends on geometry but analysis of simple cases with large carbon particles and small gaps shows that the ratio of the moduli does not have to be much larger than unity.

The real material is, of course, solid and this constrains the extent to which the two materials can respond differently. A quantitative treatment of the effect of pressure would require detailed knowledge of the material's structure. However, the above discussion provides a convincing explanation for the relatively weak response to pressure in this

particular system. It also suggests an explanation for the non-linear behaviour at higher pressures: the stresses near the small tunnel gaps between carbon particles will be large and highly non-uniform so the local response may exceed the linear limit. It would be interesting to make similar measurements on a composite in which the conducting particles were harder than the matrix.

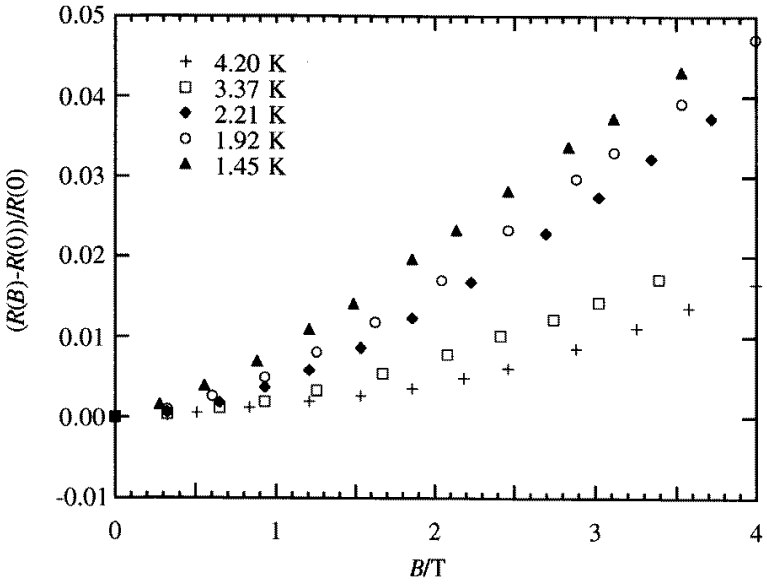

Figure 9. The magnetoresistance of EC140.

4.2.2. Magnetoresistance. The magnetoresistance (always positive) measured in EC140 at various temperatures is shown in figure 9. It may be accounted for by shrinking of the electronic wave functions by the magnetic field, as first discussed by Yafet *et al* (1956). A strong magnetic field causes a wave function to contract in the plane perpendicular to the magnetic field. In the case of localized electrons this decreases the probability of hopping occurring due to the decreased wave-function overlap between neighbouring states. The electrons are not strongly localized in the carbon black, but the magnetic field will increase α, the tunnelling exponent, and increase the sample resistance through reduction of the inter-particle tunnelling probability. Shklovskii and Efros (1984) show that if the resistance is of the form $R = R_0 \exp(2\alpha r)$ with α^{-1} being the extent of the wave function, then the magnetoresistance follows

$$\ln(R(B)/R(0)) \propto B^2$$

at very low fields, and

$$\ln(R(B)/R(0)) \propto B^{1/2}$$

at high fields. In the transition region between these limiting cases the magnetoresistance is approximately linear in field (Shklovskii and Efros 1984). The results of figure 9 are consistent with such a transition from quadratic to a linear dependence. Thus the magnetoresistance of EC140 can be explained on the basis of the shrinking of the electronic

wave functions by the field. This is consistent with the interpretation of the conductivity data, which indicates that inter-particle transport determines the conductivity.

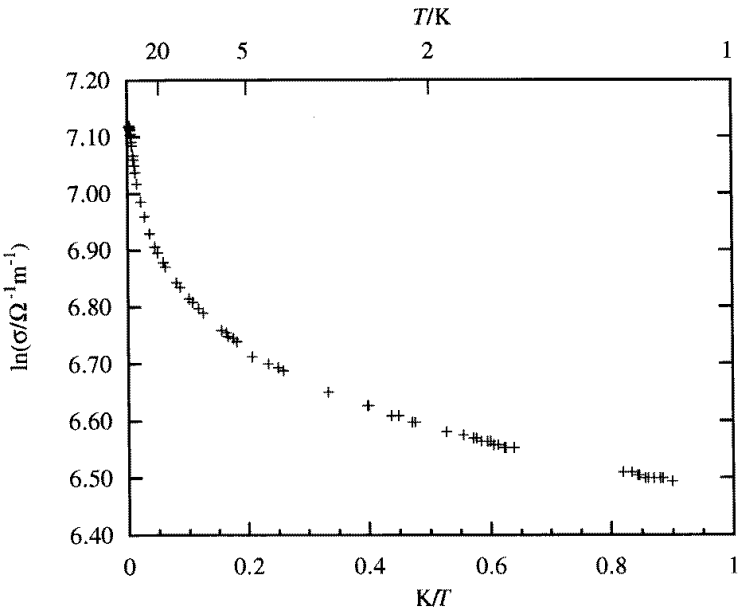

Figure 10. Temperature dependence of the conductivity of C-wax (50% XC72 carbon black in Montan wax)

4.3. Results with the highly conductive composite

4.3.1. Resistivity measurements. The conductivity of C-wax was measured down to 1.2 K. The data are plotted in figure 10 in the form $\ln\sigma$ versus T^{-1}. This obviously is not a straight line. It was also found that the data could not be described by the variable-range-hopping equation $\sigma = \sigma_0 \exp[-(T_0/T)^x]$. Although this form fitted the data over limited ranges of temperature with various values of x, T_0 was too small for the expression to be valid. For example, the data for $T < 12$ K could be fitted with $x = 1/4$, but then $T_0 = 0.4$ K, much smaller than the lowest-temperature measurement. (The form is only valid if $T_0 > T$.) Nor could the fluctuation-induced tunnelling theory be used: fitting the data to this form resulted in $T_1 < 0$ which is unphysical.

The low-temperature data are very well described however by $\Delta\sigma \propto \ln T$. This is shown in figure 11. Such a dependence is accounted for in terms of quantum corrections to resistance in a two-dimensional disordered conductor (Lee and Ramakrishnan 1985). This interpretation implies that the temperature dependence of the resistivity at low temperatures is dominated by intra-particle transport on the graphitic planes and that inter-particle transfers (which must still occur) must be relatively easy. Since the carbon black graphitic structure is imperfect compared with that of single-crystal graphite, we may expect the mean free path to be short enough for the effects of disorder to be important in determining transport within the particles.

For a two-dimensional theory to apply, the system must be two-dimensional at the characteristic scale of quantum corrections. There are two characteristic lengths—the phase-

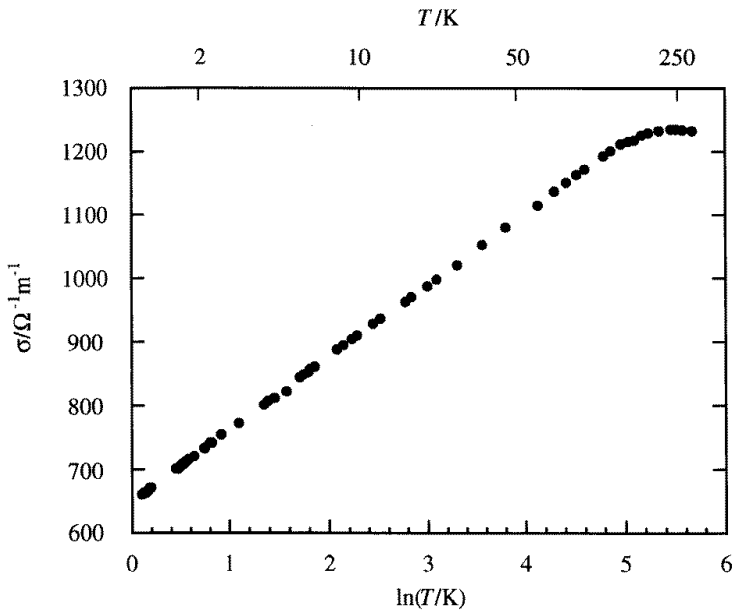

Figure 11. Conductivity of C-wax as a function of $\ln T$, showing good agreement with the predictions of disordered metallic conduction in two dimensions.

breaking length disregarding electron–electron interactions L_ϕ, and the thermal length L_T for electron–electron scattering. The latter is generally shorter but both lengths are of the order of tens of nanometres. The condition that the electrons are sufficiently confined to the graphitic planes may be expressed in terms of the in-plane and inter-layer resistances. The condition for two dimensionality requires that the in-plane sheet resistance be less than the resistance between neighbouring planes of area L_ϕ^2 or L_T^2, i.e. that the anisotropy of the graphite resistance should be larger than $L_T^2/a^2 \approx 10^3$ where a is the inter-plane separation (Astrakharchik 1995). This condition is indeed satisfied in normal graphite and so will be also in the carbon black particles provided that there are no significant extra conduction paths between planes.

The full expression for quantum corrections to conductivity in a weakly disordered two-dimensional system when spin-flip scattering is negligible, as given by Lee and Ramakrishnan (1985), is

$$\sigma(T) = \sigma(0) + \frac{e^2}{2\hbar\pi^2}(p + (1 - 0.75\tilde{F}_\sigma)) \ln\left(\frac{T}{T_0}\right) \tag{2}$$

where the inelastic scattering time τ_ϕ varies as T^{-p}, T_0 is a constant and $\tilde{F}_\sigma$ is related to the screening. The first term in parentheses is the correction due to weak localization and the second comes from electron–electron interaction effects. The index p depends on the dominant inelastic scattering mechanism which here may be electron–electron or electron–phonon collisions. Boundary scattering is assumed to cause only elastic scattering. Belitz and Das Sharma (1987) calculated τ_ϕ for thin metal films above 4.2 K. They found that the temperature dependence of the electron–phonon scattering time $\tau_\phi^{\mathrm{e-ph}}$ is not a simple power law; however over the range 4–20 K it can be approximated by $\tau_\phi^{\mathrm{e-ph}} \sim T^{-2.5}$. Including also the electron–electron process (for which alone $p = 1$) leads to an effective $p \simeq 2$ over

this range. They assumed the electron–phonon scattering to be a two-dimensional process; this is the case in graphitic carbon as the in-plane vibrations are expected to scatter the electrons most effectively. Although electron–phonon scattering is expected to be relatively weak in graphite due mainly to the small density of electron states near the Fermi energy (McClure 1964), it is unlikely that it will have no effect. Thus $p \sim 2$ would seem to be a reasonable value to use in our low-temperature analysis. As the temperature rises electron–electron scattering processes will decrease in importance relative to the electron–phonon interactions, and p might be expected to increase leading to a higher slope of σ versus $\ln T$.

The conductivity does not show a $\ln T$ dependence at temperatures above about 150 K. The expansion of the matrix may decrease the conductivity at high temperatures, as discussed for the lightly loaded composites. In order for this suggestion to be plausible the matrix must expand so much that the assumption of easy inter-particle transfers is no longer valid. In addition, the weak-localization contribution to the temperature dependence of the conductivity becomes unimportant at high temperatures as the inelastic scattering length becomes shorter than the elastic length. Eventually, at high enough temperatures the conductivity will then begin to decrease with increasing temperature due to reduction of the mean free path by normal phonon scattering processes. These processes may account for the turnover at high temperatures.

It should be noted that we have also observed the two-dimensional $\Delta\sigma \sim \ln T$ behaviour in samples of compressed carbon black with no binder. This supports our interpretation that the behaviour of the highly loaded C-wax sample derives from the intra-particle processes described above.

4.3.2. Magnetoresistance. The magnetoresistances of C-wax and of a sample of compressed carbon black were measured below 4.2 K. In both, we found positive magnetoresistance, the magnitude of the effect decreasing with increasing temperature. The results are similar to those obtained with carbon resistance thermometers (Koike *et al* 1985). These consist of graphitic grains held together by a binder and exhibit a small positive magnetoresistance above ~0.5 K; below this temperature the magnetoresistance may become negative. Koike *et al* (1985) explain their results on the basis of the theory of Yosida and Fukuyama (1980). This applies to a localized system in which the mobility edge can be shifted by the magnetic field. The C-wax sample conductivity does not indicate strongly localized behaviour and thus we look to interpret the magnetoresistance in terms of the same physics as was used to explain the conductivity data, i.e. weak localization and electron–electron interactions in a disordered two-dimensional material.

Weak localization and electron–electron interactions lead to negative and positive magnetoresistance respectively. We found only positive magnetoresistance, implying that electron–electron interaction is the dominant mechanism in this temperature range. This is a puzzling result as weak localization is normally much more sensitive to magnetic fields than electron–electron interaction terms in the conductivity. However, if we assume interaction to be the origin of the observed positive magnetoresistance, we may test the data against this model.

In two dimensions the magnetoconductivity for electron–electron interactions is of the form

$$\Delta\sigma = -\frac{e^2}{\hbar}\frac{\tilde{F}_\sigma}{4\pi^2}g_2(h) \tag{3}$$

where

$$g_2(h) = \begin{cases} \ln(h/1.3) & h \gg 1 \\ 0.084h^2 & h \ll 1. \end{cases}$$

$h = g\mu_B B/kT$ and $\tilde{F}_\sigma$ is related to the screening (Lee and Ramakrishnan 1985). The magnetoconductivity is expected to become important for $h > 1$. Taking $g = 2$, the field corresponding to $h = 1$ decreases from 3.1 T at 4.2 K to 0.87 T at 1.17 K, and this regime is therefore accessible in our measurements. The observed changes in conductivity at a number of temperatures are plotted versus $\ln B$ in figure 12. The data do go over to the form $\Delta S \propto \ln B$ at high fields, and this behaviour becomes apparent at lower fields as the temperature is lowered.

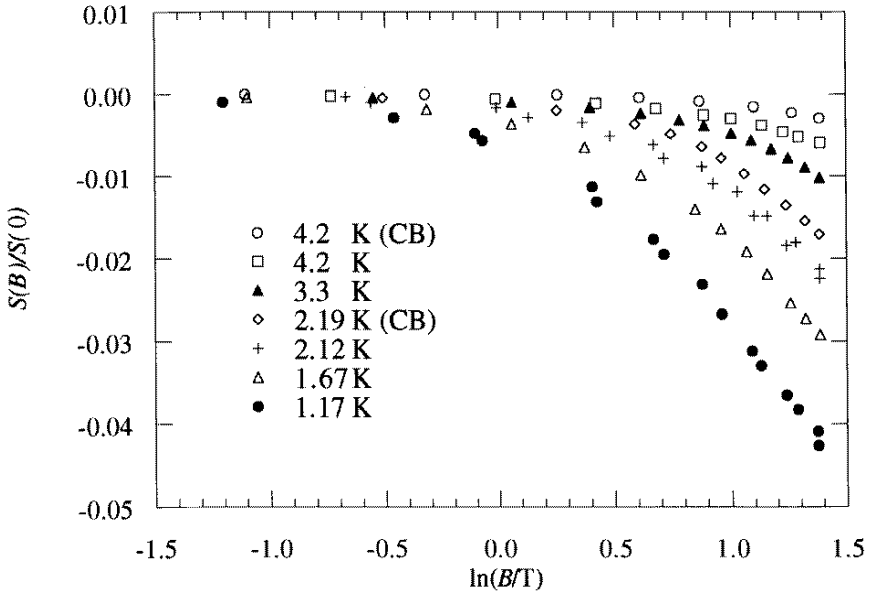

Figure 12. Magnetoconductance as a function of $\ln B$. The samples marked CB were of compressed carbon black with no binder.

From equation (3), the magnetoconductivity at constant high field should be proportional to $\ln T$. The change in conductance at 4 T is plotted as a function of $\ln T$ in figure 13 for C-wax and forms a straight line, thus verifying that this is so. The form of the results is therefore entirely consistent with the assumption that the magnetoconductance arises from the electron–electron interaction effect.

The magnitudes of these results cannot be compared directly with theory as the multiplicative factor A required to obtain the measured (three-dimensional) system conductance from the appropriate two-dimensional form is not known. However, the same factor will be involved in both conductance and magnetoconductance measurements. The conductance is given at constant magnetic field by

$$S(T) = S(T_0) + A\frac{e^2}{2\hbar\pi^2}(p + (1 - 0.75\tilde{F}_\sigma))\ln\left(\frac{T}{T_0}\right) \equiv C_T + m_T \ln T$$

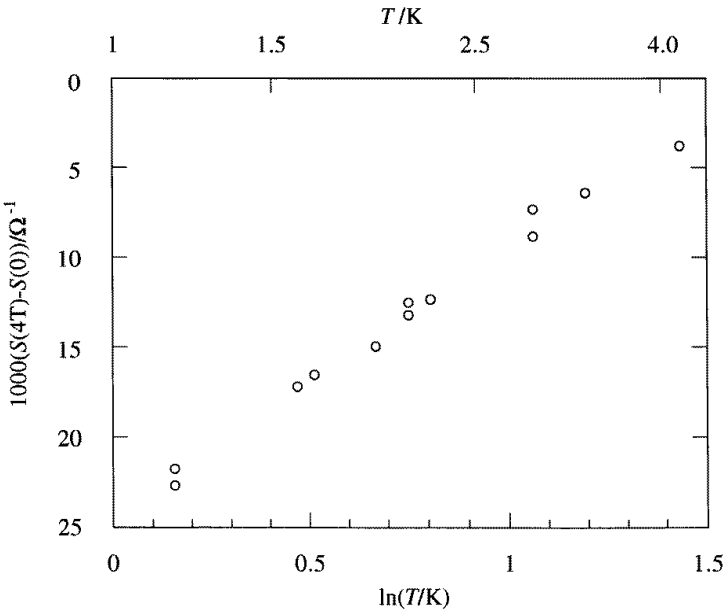

Figure 13. The change in conductance at 4 T as a function of $\ln T$ for C-wax.

while the high-field magnetoconductance is

$$\Delta S = -A\frac{e^2}{\hbar}\frac{\tilde{F}_\sigma}{4\pi^2}\ln\left(\frac{g\mu_B B}{1.3kT}\right) \equiv C_B + m_B \ln T$$

with the C_i and m_i being constant at constant field. Thus

$$\frac{m_T}{m_B} = \frac{2(p+1-0.75\tilde{F}_\sigma)}{\tilde{F}_\sigma}.$$

In our case $m_T = 0.0886 \pm 0.0002\ \Omega^{-1}$ for $T < 30$ K and $m_B = 0.0149 \pm 0.0005\ \Omega^{-1}$, giving $\tilde{F}_\sigma = 0.27(p+1)$. As discussed earlier, we expect $p \approx 2$. This gives $\tilde{F}_\sigma \approx 0.81$. This is within the bounds predicted by theory which gives $0 \leqslant \tilde{F}_\sigma \leqslant 0.8655$ (Lee and Ramakrishnan 1985), but is also quite high, indicating that interaction effects are indeed important in this system. This may help explain why we do not see the negative magnetoresistance due to weak localization. The weak-localization contribution to the magnetoresistance will also be diminished by the geometry of the situation: as only the component of the field normal to the graphitic planes is effective, there will be angular averaging within the structure. In contrast, magnetoresistance in the interaction component is isotropic.

The value of the geometric factor can now be obtained. By substituting back, one obtains $A \approx 3000$. The system effectively consists of a large number of parallel conducting two-dimensional paths, corresponding to the well defined graphitic planes forming the outer layers of the carbon black particles. Thus A should be large, as here. Our results are therefore also in quantitative agreement with the theory.

5. Conclusions

Data obtained from carbon–polymer composites containing varying amounts of carbon have been presented in this paper. The range of resistivities covered is wider than in any previous work. We have shown that two aspects to the conduction process must be considered: conduction within the carbon black particles and transfer of charge between them. As expected, the latter dominates the resistance in composites with low loading, and is satisfactorily described by the mechanism of fluctuation-induced tunnelling conduction. This mechanism together with orbit shrinkage also accounts correctly for the observed positive magnetoresistance. In highly loaded materials, transfer between particles becomes easy and resistance is dominated by intra-particle processes. These are identified as quantum corrections to conductivity in the disordered two-dimensional graphitic planes that are present in the particles of carbon black, with electron–electron interactions dominating over weak-localization effects, as is normally the case in two-dimensional disordered conductors. The magnetoresistance observed in the highly loaded materials was also found to be positive, implying that the weak-localization component is suppressed. Analysis of the magnetoresistance assuming it to come from interaction effects gives results that are qualitatively and quantitatively acceptable. We cannot explain the apparent suppression of the weak-localization component of the magnetoresistance.

Acknowledgments

We should like to thank Dr Seth of the ICI Wilton Materials Research Centre for supplying the materials studied, Ian Marsden for carrying out the high-pressure measurements, Dr E G Astrakharchik for valuable discussions and the Master and Fellows of Churchill College, Cambridge, for a Research Scholarship that supported one of us (JCD) during the course of this work.

References

Adkins C J 1982 *J. Phys. C: Solid State Phys.* **15** 7143
Aharony A, Brooks Harris A and Entin-Wohlman O 1993 *Phys. Rev. Lett.* **70** 4160
Al-Allak H M, Brinkman A W and Woods J 1993 *J. Mater. Sci.* **28** 117
Astrakharchik E G 1995 private communication
Belitz D and Das Sharma S 1987 *Phys. Rev.* B **36** 7701
Bolz R E and Tuve G L (ed) 1973 *CRC Handbook of Tables for Applied Engineering Science* 2nd edn (Boca Raton, FL: Chemical Rubber Company Press)
Brydson J A 1982 *Plastics Materials* 4th edn (London: Butterworths)
Burgess K A, Scott C E and Hess W M 1971 *Rubber Chem. Technol.* **44** 230
Deutscher G, Lévy Y and Souillard B 1987 *Europhys. Lett.* **4** 577
Ergun S 1970 *Phys. Rev.* B **1** 3371
Ezquerra T A, Baltá Calleja F J and Plans J 1986 *J. Mater. Res.* **1** 510
Fabish T J and Schleifer D E 1984 *Carbon* **22** 19
Koike Y, Fukase T, Morita S, Okamura M and Mikoshiba N 1985 *Cryogenics* **25** 499
Lee P A and Ramakrishnan T V 1985 *Rev. Mod. Phys.* **57** 287
McClure J W 1964 *IBM J. Res. Dev.* **8** 255
Mehbod M, Wyder P, Deltour R, Pierre C and Gueskens G 1987 *Phys. Rev.* B **36** 7627
Norman R H 1970 *Conductive Rubbers and Plastics* (Amsterdam: Elsevier)
Ohe K and Naito Y 1971 *Japan. J. Appl. Phys.* **10** 99
Parker I D 1988 *PhD Thesis* University of Cambridge
Robertson J 1986 *Adv. Phys.* **35** 317
Sheng P 1980 *Phys. Rev.* B **21** 2180

Sheng P and Klafter J 1983 *Phys. Rev.* B **27** 2583
Sheng P, Sichel E K and Gittleman J I 1978 *Phys. Rev. Lett.* **40** 1197
Shklovskii B I and Efros A L 1984 *Electronic Properties of Doped Semiconductors* (Berlin: Springer)
Sichel E K (ed) 1982 *Carbon Black–Polymer Composites (Plastics in Engineering 3)* (New York: Dekker)
Van der Putten D, Moonen J T, Brown H B, Brokken-Zijp J C M and Michels M A J 1992 *Phys. Rev. Lett.* **69** 494
Warren B E 1941 *Phys. Rev.* **59** 693
Yafet Y, Keyes R W and Adams E N 1956 *J. Phys. Chem. Solids* **1** 137
Yosida K and Fukuyama H 1980 *J. Phys. Soc. Japan* **48** 1879